ACS Sustainable Chemistry & Engineering

pubs.acs.org/journal/ascecg

Research Article

Biobased Ultralow-Density Polyurethane Foams with Enhanced Recyclability

Olga Gotkiewicz, Mikelis Kirpluks, Zuzana Walterová, Olga Kočková, Sabina Abbrent, Paulina Parcheta-Szwindowska, Ugis Cabulis, and Hynek Beneš*

Cite This: *ACS Sustainable Chem. Eng.* 2024, 12, 1605−1615

Read Online

ACCESS | Metrics & More | Article Recommendations | Supporting Information

ABSTRACT: Polyurethane (PUR) foams are widely used in many engineering applications, but their efficient recycling has remained a major challenge for many years. This study presents a novel strategy of incorporating hydrolyzable ester units into the PUR structure to enhance PUR foam recyclability. The present eco-design concept of PUR materials enables fully the replacement of petrochemical polyols with biobased alternatives and production of ultralow-density (16 kg·m^{-3}) PUR foams. To reach this target, a series of low-function polyols based on succinic acid (SA) were first synthesized. Their subsequent use in combination with a high-functional biobased tall oil-derived polyol led to the production of highly homogenous semirigid, partly open-cell PUR foams with outstanding structural, thermal, and mechanical properties. Additionally, the study shows that the incorporation of SA-polyols with hydrolyzable ester linkages into the PUR foams significantly enhances their recyclability via glycolysis, proving their potential in contributing to a circular economy and addressing plastic waste concerns.

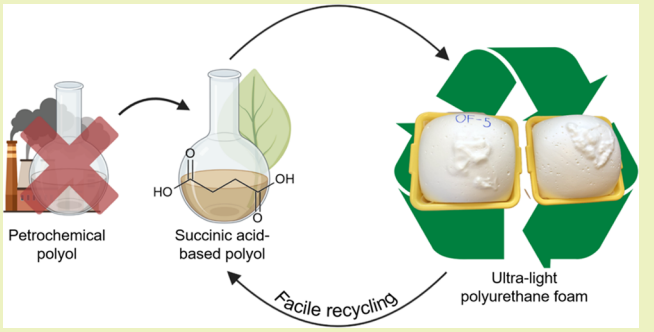

KEYWORDS: *polyurethane, foam, recycling, biobased, solvolysis*

INTRODUCTION

Although there is a current increased interest in the issue of plastic recycling and novel recycling methods are constantly being developed, the plastic recycling rate of 16.4% is disappointingly low.[1] Due to today's highly demanding transformation to a circular economy and the achievement of targeted recycling quotas, the concept of eco-design of polymer materials needs to be introduced in order to effectively transform plastic waste into valuable feedstock. This is particularly important for thermosets due to their permanently cross-linked structure that cannot be melted and reshaped. Thermosets are widely used in many applications, e.g., construction, automotive, and packaging sectors, accounting for approximately 12% of global plastic production (44 million tons).[2] Particularly, polyurethane (PUR) foams are, due to their high tunability and versatility, unambiguously the most produced thermosets (ca. 25.8 million tons in 2022).[3] This huge production creates an urgent demand for sustainable solutions for PUR foams, which would meet the requirements of circular economy, namely durability, reusability, and recyclability.[4]

Considering sustainable development goals to reduce environmental impact, it is expected that low-density PUR foams (20−40 kg·m^{-3}) currently holding the largest share of the PUR foam market[5−7] will be replaced by partly open-cell PUR foams with an even lower density (<20 kg·m^{-3}) in the near future. These ultralow-density PUR foams are nowadays a rapidly emerging class of sustainable materials with unique advantages such as very low weight, resulting in low-cost materials, good thermal insulation, sound absorption, and vibration dampening properties.[8,9]

To achieve the circular economy goals, the macromolecular design of PUR foams has to be better adapted to end-of-life treatment, enabling facile recycling via solvolytic degradation.[10] PUR foams are generally obtained by the step-growth polymerization of polyisocyanates and polyols. Tailor-made polyester polyols bearing hydrolyzable ester groups[11] are key for the fabrication of PUR foams with enhanced degradability.[12] Additionally, introducing hydrophilic entities such as glycol chains into the PUR structure can further accelerate the degradation rate.[13−15]

On the other hand, current environmental regulations have prompted an increased demand for environmentally friendly alternatives. Nowadays, the raw materials associated with the production of polyester polyols are mostly of petrochemical

Received: October 23, 2023
Revised: January 2, 2024
Accepted: January 3, 2024
Published: January 16, 2024

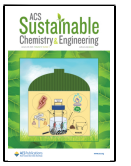

https://doi.org/10.1021/acssuschemeng.3c06924
ACS Sustainable Chem. Eng. 2024, 12, 1605−1615

Table 1. Formulations of the Prepared PUR Foams Including Proportions of Polyols

PUR foam ID	proportions of polyols, wt %						proportions of PUR foams, wt %		
	SA-diol	SA-triol	SA-tetraol	ETO-TMP	Lupranol 3422	Lupranol 1100	polyols	pMDI	other[a]
REF	0	0	0	0	20	80	22	60	18
1-PU-diol	80	0	0	0	20	0	24	58	18
1-PU-triol	0	80	0	0	20	0	23	59	18
1-PU-tetraol	0	0	80	0	20	0	23	59	18
2-PU-diol	80	0	0	20	0	0	24	58	18
2-PU-triol	0	80	0	20	0	0	24	58	18
2-PU-tetraol	0	0	80	20	0	0	23	59	18
3-PU-diol	100	0	0	0	0	0	25	56	19
3-PU-triol	0	100	0	0	0	0	25	56	19
3-PU-tetraol	0	0	100	0	0	0	24	57	19

[a]Includes water (3.5 wt %), TCPP fire retardant (9.2−9.9 wt %), Polycat NP 10 (0.7 wt %) and DBTDL (0.03 wt %) catalysts, Niax Silicone L-6915 (2.0 wt %), and Adamantan SFOF (2.8−3.0 wt %) surfactants.

origin. Therefore, extensive research has been conducted in both academic and industrial sectors to explore the production of polyols from biomass (biopolyols). Various renewable resources, including vegetable oils, microalgae, lignocellulose, and polysaccharides, have been investigated for their potential in polyol synthesis.[16,17] Among these environmentally friendly feedstocks, succinic acid (SA) has emerged as the most suitable raw material for polyol production.[18] SA can be efficiently produced through the fermentation process of carbohydrates.[19] Furthermore, SA is found in all living organisms, where it plays a vital role in biological processes as an intermediate product in the tricarboxylic acid cycle (TCA) and is fully biocompatible.[20] The significance of SA was recognized by the US Department of Energy in 2004, which identified it as one of the top 12 value-added platform chemicals derived from biomass.[21] Additionally, SA is a key component in the manufacturing of essential industrial products such as biodegradable polymers, surfactants, detergents, food additives, pharmaceuticals, fungicides, and herbicides.[22]

Biopolyols have demonstrated their potential as valuable constituents for the production of rigid and semirigid open-cell PUR foams.[8] For example, Marcovich et al. achieved successful results by blending up to 70% of a biopolyol derived from palm oil with a petrochemical polyol to obtain semirigid PUR foams, which exhibited relatively low apparent density ranging from 29 to 35 kg·m^{-3}.[23] Similarly, Polaczek et al. prepared partially palm oil-based open-cell PUR foams with even lower apparent densities ranging from 13.0 to 15.2 kg·m^{-3}.[24] However, the incorporation of vegetable oil-derived biopolyols (without easily cleavable units) into the PUR foam structure does not improve the recyclability of the foam.

In this work, we have designed and prepared ultralow-density (15−17 kg·m^{-3}) PUR foams with incorporated hydrolyzable ester units derived from renewable SA with the aim to enhance the foam recyclability via solvolysis (glycolysis). First, a series of biobased polyester polyols with different functionalities based on SA and tetraethylene glycol (4EG) were synthesized. The obtained SA-polyols were analyzed in detail and then used for the preparation of ultralow-density (16 kg·m^{-3}), partly open-cell semirigid PUR foams. Three series of foams were compared—one based fully on the SA-polyols (diol, triol, and tetraol) and two in which SA-polyols were combined with two different polyols of higher functionality, one (commercial) of petrochemical and one of biobased (tall oil-derived) origin. The complete replacement of petrochemical polyols with the biobased varieties was studied in order to produce PUR foams with a fine and homogenous cellular structure and excellent mechanical and thermal properties while maintaining a favorable low apparent density. Finally, the glycolysis of PUR foams was studied in order to verify the improvement of their recyclability due to the presence of hydrolyzable ester bonds.

EXPERIMENTAL SECTION

Synthesis of Biobased Succinic Acid-Derived Polyols. Biobased poly(ester-ether) polyols were synthesized using a melt polycondensation method from succinic acid (SA, 99%, Sigma-Aldrich) and tetraethylene glycol (4EG, 98%, Sigma-Aldrich) using trimethylolpropane (TMP, ≥98%, Sigma-Aldrich) and pentaerythritol (98%, Sigma-Aldrich) as branching agents. The reaction was conducted in a 1 L three-neck flask equipped with a nitrogen inlet, magnetic stirrer, condenser, and thermometer. The proper amounts of SA and alcohols (OH/COOH molar ratio of 1:1) were charged into the flask and heated to 170 °C until the complete dissolution of the reactants. Subsequently, the catalyst, dibutyltin dilaurate (DBTDL, 99%, Sigma-Aldrich), was added and after ca. 5 h, the temperature was raised to 190 °C. After more than 90% of the theoretical amount of water was distilled out, the pressure was gradually reduced to ∼20 Torr. The polycondensation was stopped when the desired acid (<5 mgKOH/g) and hydroxyl (20−50 mgKOH/g) numbers were reached. Three SA-derived polyols (SA-diol, SA-triol, and SA-tetraol) differing in the hydroxyl number and functionality were synthesized; their formulations are given in Table S1.

Synthesis of the Biobased ETO-TMP Polyol. The ETO-TMP polyol was obtained from epoxidized high-oil fatty acids. The epoxidation procedure has been described in a previous study by Kirpluks et al.[25] The epoxy groups of the epoxidized tall oil fatty acids were opened with TMP (reagent grade, 97%, Sigma-Aldrich). Furthermore, a subsequent esterification reaction of the free carboxylic groups of epoxidized tall oil fatty acids was carried out.

The ETO-TMP polyol synthesis procedure was as follows. Epoxidized tall oil fatty acid (300 g) was added via a dropping funnel into a four-neck flask (1 L) already containing the mixture of TMP (the ratio of epoxidized tall oil fatty acid oxirane and carboxyl groups to TMP moles was 1:1). The tetrafluoroboric acid solution (48 wt % in H_2O, 0.3 wt % from epoxidized tall oil fatty acid) was used as a catalyst. The temperature was maintained at 80 °C during the addition of the epoxidized tall oil fatty acid by using an oil bath. In this step, the oxirane rings were opened. After all of the epoxidized oil had been added, the temperature was raised to 180 °C. The stirring was ensured with an anchor-type stirrer at 500 rpm. The water formed during the synthesis was removed with an inert carrier gas (nitrogen) and was condensed in a Liebig condenser. The duration of the synthesis was 6 h.

Preparation of Polyurethane Foams. First, a polyol part (component A) composed of polyols, distilled water (chemical

https://doi.org/10.1021/acssuschemeng.3c06924
ACS Sustainable Chem. Eng. 2024, 12, 1605−1615

blowing agent), DBTDL and Polycat NP10 (Air Products) catalysts, Niax Silicone L-6915 (Momentive Performance Materials) and Adamantan SFOF (kindly supplied by ADAMANTAN, Latvia) surfactants, and tris(1-chloro 2-propyl)phosphate (TCPP, Lanxess) fire retardant were homogenized for 5 min at 10,000 rpm using a high-shear mixer until the mixture was fully homogenous. Then, polyisocyanate (pMDI, component B) was quickly added, and the mixture was homogenized for 10 s with a mechanical stirrer at 2000 rpm. The PUR reacting mixture was then poured into the open-top mold (250 mm × 250 mm × 120 mm). To finish the cross-linking reaction, PUR foams were conditioned at room temperature for 18 h. The complete formulations of all prepared foams are shown in Table S2. All PUR foams were produced using a fixed NCO/OH ratio of 1.0.

In total, three different series of PUR foams were prepared using synthesized SA-polyols (Table 1). In the first series, denoted as 1-PU, the SA-polyols were added as a full replacement (80 wt %) for the low-functional commercially available petrochemical polyol Lupranol 1100 (BASF) with a hydroxyl number of 104 mg KOH/g and similar characteristics, while the residual 20 wt % was composed of high-functional commercially available Lupranol 3422 (BASF) with a hydroxyl number of 490 mg KOH/g and functionality of 5. In the second series, denoted as 2-PU, both petrochemical polyols, Lupranol 1100 and Lupranol 3422, were replaced by biobased analogues, i.e., the low-functional SA-polyols and the high-functional ETO-TMP, respectively. The third series, denoted as 3-PU, was fully based on the SA-polyols (free of high-functional polyols). As a reference PUR foam (denoted as REF), the formulation based entirely on commercial petrochemical polyols Lupranol 1100 and Lupranol 3422 was used.

Chemical Recycling of Polyurethane Foams. Microwave-accelerated chemical recycling (solvolysis) of the prepared PUR foams was performed without the addition of any catalyst in a monomodal microwave reactor Discover SP Microwave synthesizer (CEM Corporation) operating at 2450 MHz frequency. The mixture of fragmented PUR foams and 4EG in different weight ratios (from 1:2 to 1:1) was placed into a 50 mL glass reaction vessel together with a magnetic stirrer and then sealed tightly with a PTFE-coated silicone septum. The reaction mixture was heated using fixed power mode (150 W) until the target reaction temperature (220 °C) was reached. Then, the reaction was allowed to continue isothermally at 220 °C until the complete dissolution of the PUR foam. After the reaction was stopped, the vessel in the reactor was cooled to ambient temperature using compressed air. The reaction time was determined as the time from the start of heating to the complete dissolution of the PUR foam, i.e., full transformation into the liquid state.

Characterizations. The acid number was determined by volumetric titration according to ASTM D 4662-93. The conversion of carboxylic acid groups (COOH conversion) during polycondensation was calculated according to the following eq 1

$$\text{COOH conversion (\%)} = 100 \times [1 - n(\text{COOH})/n_0(\text{COOH})] \quad (1)$$

where n_0(COOH) and n(COOH) are moles of COOH groups before and after the polycondensation, respectively.

The hydroxyl number was determined according to ISO 2554:1974.

The water content was determined using the Karl Fischer titration method according to ISO 760.

Viscosity was measured using a Physica MCR 501 (Anton Paar, Austria) with cone/plate geometry (25 mm diameter, 2° angle, 0.15 mm gap) at a temperature of 25 °C in the range of shear rates of 0.01−100 s^{-1}.

FTIR spectra were recorded on a Spectrum 100 spectrometer (PerkinElmer) equipped with a universal ATR accessory with a diamond prism. Spectra were recorded in the wavenumber range of 650−4000 cm^{-1} over four scans with a resolution of 4 cm^{-1}.

Size exclusion chromatography (SEC) was carried out using a Modular GPC system equipped with an Evaporative Light Scattering Detector PL ELS 1000 (Polymer Laboratories), a UV detector Chrom uvd 250 operated at λ = 264 nm, and a set of two columns, PLgel MIXED-B LS, 7.5 mm × 300 mm and 10 μm (Polymer Laboratories). Tetrahydrofuran (THF) was used as a mobile phase (flow rate of 0.5 mL·min^{-1}). Calibration was performed by using PS standards.

MALDI-TOF mass spectra were obtained with an UltrafleXtreme instrument (Bruker Daltonics, Bremen, Germany) in positive ion reflectron mode. The spectra were the sum of 25,000 shots with a DPSS, Nd:YAG laser (355 nm, 2000 Hz). Delayed extraction and external calibration were used. The samples were prepared by the dried droplet method: solutions of the sample (10 mg·mL^{-1}) and of DHB (2,5-dihydroxybenzoic acid; Sigma-Aldrich, 98%, 20 mg·mL^{-1}) as a matrix with the solution of sodium trifluoroacetate ($NaCF_3COO$; Sigma-Aldrich, 10 mg·mL^{-1}) as a cationization agent in THF (Sigma-Aldrich, ≥99.9%) were mixed in the volume ratio of 4:20:1. 1 μL of the mixture was deposited on the ground steel target plate. The drop was dried in an ambient atmosphere.

Differential scanning calorimetry (DSC) was conducted using a Q 2000 calorimeter (TA Instruments). Measurements were performed in heating−cooling−heating cycles from −80 to +150 °C at a heating rate of 10 °C·min^{-1} in a nitrogen atmosphere. The glass transition temperature (T_g) was determined from the second heating cycle.

The foaming process was analyzed using a FOAMAT 285 (Format-Messtechnik GmbH, Karlsruhe, Germany). The rise profile was measured with an ultrasonic sensor, and the temperature during the foaming process was monitored using a thermocouple.

The apparent density of PUR foams was determined according to ISO 845. The obtained result is an average of six measurements.

The open cell content was determined using an Ultrapyc 5000 Foam gas pycnometer from Anton-Paar (Graz, Austria). The following measurement settings were applied: gas: nitrogen; target pressure: 3.0 psi; foam mode: on; measurement type: corrected; flow direction: sample first; temperature control: on; target temperature: 20.0 °C; flow mode: monolith; cell size: large; preparation mode: flow; and time of the gas flow: 0.5 min.

The thermal conductivity coefficient (λ) was measured by using a Linseis Heat Flow Meter 200 (Germany). The temperature of the cold plate was set to 0 °C with that of the warm plate set to 20 °C. The typical precision of the measurements was $\lambda \pm 1\%$.

The compression test was performed on cube-shaped specimens (50 mm × 50 mm × 40 mm) using an Instron 6025/5800R apparatus (Instron Limited, United Kingdom) according to ISO 844. The obtained results are an average of 10 separate measurements; for each series of specimens, a standard deviation was determined. The tests were performed at room temperature in a parallel direction to the foam rise at the speed of 5 mm·min^{-1}. The compressive modulus and compressive stress at 10% strain, taken as compressive strength, were evaluated and normalized to the specific apparent density of the reference PUR foam (16 kg·m^{-3}) according to equations[26]

$$E_{\text{norm}} = E_{\text{exp}}\left(\frac{16}{\rho}\right)^{1.7} \quad (2)$$

$$\sigma_{\text{norm}} = \sigma_{\text{exp}}\left(\frac{16}{\rho}\right)^{2.1} \quad (3)$$

where E_{exp} is the measured compressive modulus, σ_{exp} is the measured compressive strength, and ρ is the apparent density of the foams.

The data from the compression test and the apparent density measurement were statistically evaluated using a one-way analysis of variance (ANOVA) for each foam series (1-PU, 2-PU, and 3-PU) with the functionality of SA-polyols as a factor.

Thermogravimetric analysis (TGA) was conducted using a Pyris 1 TGA (PerkinElmer). The samples were heated from 35 to 800 °C under a nitrogen flow at a rate of 10 °C·min^{-1}.

Scanning electron microscopy (SEM) images of the PUR foams were obtained using a Vega Plus TS 5135 (Tescan, Czech Republic) using secondary electron imaging (SEM/SE) at 30 kV. The samples were cut at room temperature, perpendicular to the foam rise direction, then fixed on a metallic support with silver-based adhesive, and sputtered with gold for 360 s in a high-vacuum sputter coater

https://doi.org/10.1021/acssuschemeng.3c06924
ACS Sustainable Chem. Eng. 2024, 12, 1605−1615

Leica EM SCD050 (Leica Microsystems, Germany). The captured images (in a direction perpendicular to the foam rise) were analyzed to measure the average cell size and cell size distribution using ImageJ 1.54f software by manual counting of 400 cells.

RESULTS AND DISCUSSION

Characterization of Biobased Poly(ester-ether) Polyols. The synthesized SA-polyols were primarily designed to enhance the (bio)degradability and chemical recyclability of the PUR foams. Therefore, the hydrolyzable ester group was introduced into the structure of the synthesized polyols[27] by the reaction of SA and 4EG. The progress of polycondensation was followed by FTIR spectroscopy and acid number determination. The FTIR spectra of all synthesized SA-polyols show in the region of C═O vibrations only one dominant band of ester groups at 1730 cm^{-1} (Figure S1), which indicates the completed polycondensation reaction. Acid number determination (Table 2) showed ∼99% conversion of COOH groups for all SA-polyols and thus almost complete esterification of SA.

Table 2. Characteristics of the Prepared SA-Polyols

	SA-diol	SA-triol	SA-tetraol
hydroxyl number, mg KOH·g^{-1}	20 ± 3	30 ± 2	50 ± 3
acid number, mg KOH·g^{-1}	4.7 ± 0.1	5.3 ± 0.9	3.1 ± 0.1
COOH conversion, %	98.6	98.5	99.1
T_g, °C	−39	−37	−37
viscosity at 23 °C, mPa·s	13,000 ± 1000	29,000 ± 2000	51,000 ± 1000
M_n[a], g·mol^{-1}	5610	5610	4490
M_w[b], g·mol^{-1}	5700	6800	11,600
$Đ$	2.0	2.4	3.7
f_n (targeted)	2	3	4
water content, wt %	0.12 ± 0.01	0.15 ± 0.01	0.21 ± 0.02

[a]Calculated from the structure. [b]Molecular weights determined by SEC are approximate values to PS standards.

Since the SA-polyols are intended for use as the main polyol component of PUR foams, it was necessary to keep their key processing parameters (mainly viscosity) similar to those of the petrochemical (polyether) polyols. However, it is known that polyester polyols generally exhibit high viscosity and a tendency to crystallize, which limit their use for PUR foams.[28] For example, a commercially available polyester polyol based on SA and 1,3-propanediol (PDO) is a solid at room temperature with a melting point of 48 °C and a viscosity of 1960 mPa·s at 70 °C,[29] which practically excludes its application for PUR foams. Similarly, the semicrystalline character and high melting point (103 °C) of the SA/1,4-butanediol polyester polyol require PUR foaming at elevated temperatures.[30] Therefore, our strategy involved the incorporation of three flexible ether linkages into each constitutional repeating unit of SA-polyols, causing a substantial flexibility increase in the polyol chains. This approach allowed us to suppress the crystallization tendency and obtain fully amorphous (low-T_g) SA-polyols with acceptable viscosities (Table 2). Thus, the designed polyols showed viscosities in the range of 13−51 Pa·s at 23 °C, permitting the subsequent PUR foaming step to be conducted at room temperature. The viscosity of the linear SA-diol was significantly lower compared to that of SA-triol and SA-tetraol containing three and four functional branching units, respectively. This increase in viscosity corresponded to increasing molecular weight (especially M_w values) of polyols in the order SA-diol < SA-triol < SE-tetraol (Figure S2 and Table 2) as well as to previous studies reporting that polyols with low functionality and a low hydroxyl number reach lower viscosities than those of polyols having high functionality and/or a high hydroxyl number.[31]

Long-chain polyols with low functionality typically induce a delay in the gelation point during the cross-linking reaction,[28,32] which in consequence promotes cell rupture during foaming and leads to the formation of PUR foams with open cells. Since the purpose of this work is to apply the synthesized SA-polyols for the preparation of semirigid, open-cell PUR foams, the condensation was carried out to a relatively high degree, ensuring that the resulting SA-polyols exhibited a high molar mass (around 5000 g·mol^{-1}), a low hydroxyl number (ca. 30−50 mg KOH·g^{-1}), and a targeted average functionality of 2, 3, and 4 (Table 2). The SA-diol was formulated as an aliphatic diol with a fully linear structure. Although two-functional polyols can be successfully used for polymer network buildup, such PUR foams purely based on diols usually have inferior mechanical properties and poor dimensional stability. Therefore, polyols with functionality above 2 are usually attempted, which is, however, often impossible in the case of polyester polyols as it is associated with a dramatic increase in viscosity. In our case, however, thanks to the presence of flexible 4EG units reducing the polyol viscosity, the synthesis of SA-triol and SA-tetraol, both liquid at room temperature, was successfully carried out (Table 2). The branched structures of SA-triol and SA-tetraol have been obtained thanks to the addition of a certain amount of three and four functional alcohols (Table S1) acting as branching units.

MALDI TOF mass spectrometry enabled the identification of chemical structures in the prepared SA-polyols. All spectra show the presence of one dominant distribution of molecular ions (ionized by Na^+) containing the SA-4EG repeating unit ($\Delta m/z$ = 276 Da) and with peak positions revealing a linear structure with two OH terminal groups (Figures S3−S5). Besides this main distribution of the targeted diol structure, minor distributions with the same mass increment of 276 Da were identified. These less-intensive distributions indicate the formation of condensation byproducts with linear structures terminated by −OH and −COOH groups as well as cyclic structures. Furthermore, in the case of SA-triol and SA-tetraol, MALDI TOF mass spectrometry revealed the formation of targeted branched SA-4EG structures derived from trimethylolpropane (SA-triol) and pentaerythritol (SA-tetraol) branching units.

Preparation of Polyurethane Foams. Three series of PUR foams were prepared with different polyol compositions. The first series (1-PU series) was derived from a standard formulation of a semirigid, open-cell PUR foam (see the reference PUR foam denoted as REF). A major part of polyols (80 wt %) consisting of a low-functional commercial petrochemical polyol, Lupranol 1100, was replaced by the low-functional biobased SA-polyols and the residual 20 wt % contained a high-functional commercial petrochemical polyol (Lupranol 3422). In the second series of PUR foams (2-PU series), both petroleum-based polyols were replaced by

https://doi.org/10.1021/acssuschemeng.3c06924
ACS Sustainable Chem. Eng. 2024, 12, 1605−1615

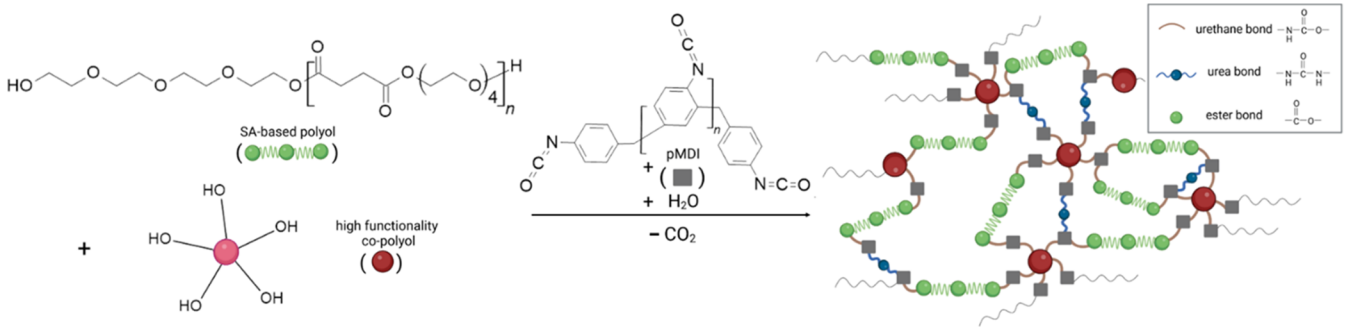

Figure 1. Schematic illustration of the PUR foam chemistry and the structure of the formed PUR foam.

biobased varieties, with 80 wt % of the low-functional SA-polyols and 20 wt % of high-functional ETO-TMP polyol. The third series of PUR foams (3-PU series) was prepared with the aim of verifying the possibility to obtain mechanically robust PUR foams based exclusively on the low-functional biobased SA-polyols.

The petrochemical polyols were replaced by bioanalogues (SA-based or ETO-TMP polyols) with similar characteristics (hydroxyl number and functionality). In this way, the mass proportion of polyol/pMDI and the amount of water (chemical blowing agent) were kept constant for all prepared PUR foams (Table 1), thereby avoiding the influence of different amounts of pMDI on the foam properties.[33] A stoichiometric NCO/OH molar ratio of 1:1 in all PUR foams meant that each hydroxyl group would react with one isocyanate group and form urethane linkages, as depicted in Figure 1. The second main component, water, acts as a chemical blowing agent and is primarily responsible for foam formation, while no additional physical coblowing agents need to be used. Upon mixing the formulation, water reacts with pMDI to form CO_2 and the disubstituted ureas (Figure 1).

After intensive mixing of all components, the PUR formulation creamed for ~30 s and then rose within 57−95 s (Table 3). The foaming reaction began the fastest for the foams containing SA-tetraol (1-PU-tetraol, 2-PU-tetraol, and 3-PU-tetraol) characterized by the highest content of hydroxyl groups, but they also exhibited the lowest rising rate attributed to their more branched structure causing lower mobility as well as resulting in higher steric hindrance compared to SA-diol and SA-triol.[8] No significant differences were found in the cream times of PUR foam formulations with SA-diol and SA-triol. The addition of SA-polyols to the PUR foam formulation slightly accelerated the foaming process (in comparison to REF), except for the series 3-PU containing only low-functional SA-polyols. In this case, the foam rise was the slowest due to the formation of more diluted PU networks with prolonged gel times. In contrast, the addition of ETO-TMP polyol slowed down the foaming due to the presence of both less reactive secondary OH groups and sterically hindering OH groups on the polyol branches (more about the ETO-TMP structure can be found in ref 25).

Table 3. Foaming Parameters (Cream and Rise Times) of PUR Foams' Formulations

PUR foam	cream time, s	rise time, s
1-PU-diol	31 ± 4	57 ± 10
1-PU-triol	35 ± 8	67 ± 9
1-PU-tetraol	29 ± 6	64 ± 11
2-PU-diol	27 ± 4	72 ± 11
2-PU-triol	29 ± 7	67 ± 17
2-PU-tetraol	25 ± 7	71 ± 10
3-PU-diol	31 ± 2	84 ± 5
3-PU-triol	34 ± 1	92 ± 1
3-PU-tetraol	31 ± 1	95 ± 4
REF	27 ± 1	81 ± 3

The FTIR spectra of the obtained PUR foams show all bands typical for linkages in the PUR foams: N−H stretching vibrations at 3340 cm^{-1}, C═O stretching vibrations corresponding to urethane and ester (1750 cm^{-1}) and disubstituted urea (1600 cm^{-1}) linkages, and N−H and C−N vibrations of urethane and disubstituted urea bonds at ~1500 cm^{-1} (Figure S6).[34] A characteristic band for N═C═O groups at 2300 cm^{-1} reflects the presence of unreacted isocyanates due to the incomplete reaction. Unreacted isocyanate groups are a typical feature of rigid and semirigid PUR foams undergoing vitrification during the cross-link reaction due to steric hindrance of the reactive sites preventing a complete reaction between the isocyanate and hydroxyl groups.[35]

Morphology of Polyurethane Foams. SEM micrographs presented in Figure 2 show a homogenous cellular structure with an average cell diameter in the range of 170−370 μm (Figure S7) for all SA-polyol-based PUR foams. With increased SA-polyol functionality, the cell diameter is shown to decrease, while the PUR foams become more homogenous. Following the theory of cross-linking stating that the higher the polyol functionality, the faster the increase in viscosity and the formation of a gel (infinite polymeric network),[36] bubble degradation via coalescence and/or Ostwald ripening was reduced due to the rapid increase in the viscosity of the reactive mixture,[37] resulting in smaller cell sizes, especially for PUR foams based on the tetra-functional polyol (SA-tetraol). Changes in the microstructure were most probably caused by the viscosity of the SA-tetraol. Its addition to the polyol part resulted in an overall increase in the viscosity of the reaction PUR mixture, which reduced the coalescence among bubbles, thereby decreasing the cell size of the foams and increasing the number of foam cells.[38] The partly open-cell structure of all PUR foams is visible in SEM micrographs under enhanced magnification (Figure S8), showing the formation of partially opened, pinhole-containing, and closed cell membranes. The content of open cells in the PUR foams ranges from 40 to 60% (Table S4) regardless of the composition.

Mechanical Properties of Polyurethane Foams. All PUR foams were prepared as large blocks (about 6000 cm^3) and then cut into cube-shaped specimens for mechanical

https://doi.org/10.1021/acssuschemeng.3c06924
ACS Sustainable Chem. Eng. 2024, 12, 1605−1615

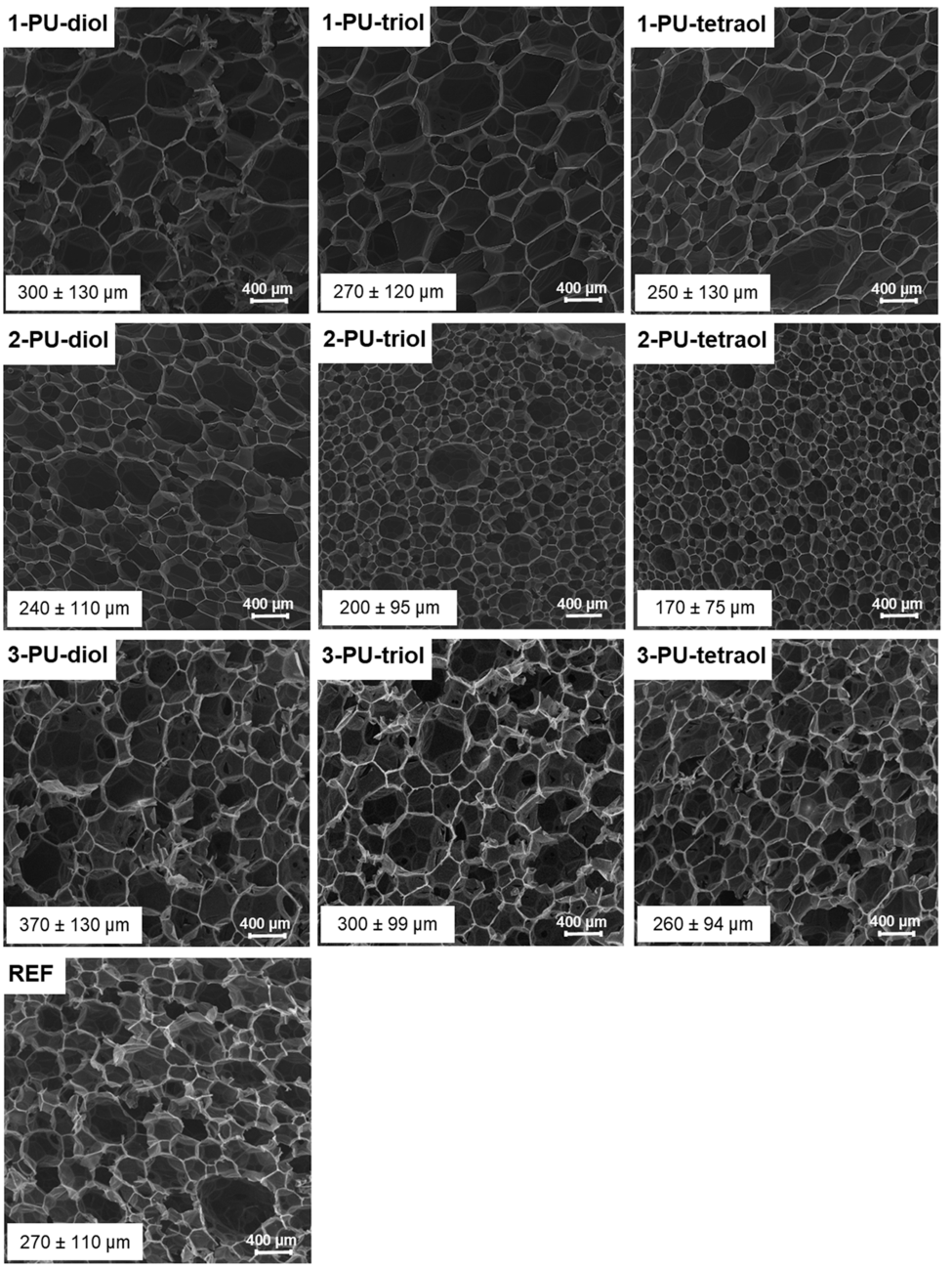

Figure 2. SEM micrographs of PUR foams taken in the perpendicular direction to foam rise. Average cell sizes are given in the lower left corners of each image.

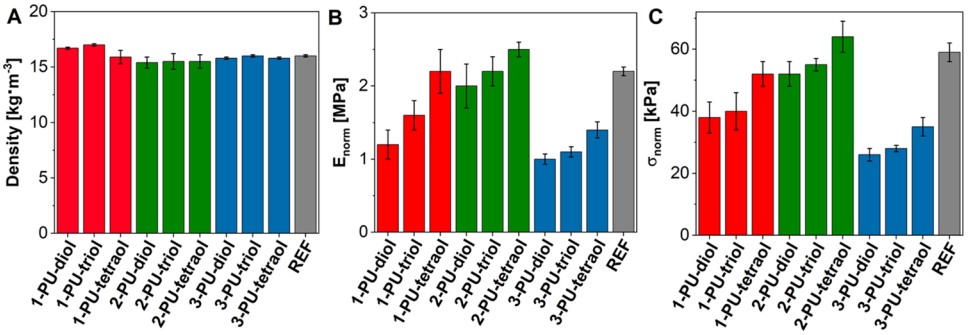

Figure 3. (A) Free rise density, (B) compressive modulus (E_{norm}), and (C) compressive strength (σ_{norm}) of the prepared PUR foams measured in the parallel direction to foam rise and normalized to the density of 16 kg·m^{-3}.

https://doi.org/10.1021/acssuschemeng.3c06924
ACS Sustainable Chem. Eng. 2024, 12, 1605−1615

Table 4. Thermal Properties of PUR Foams[a]

PUR foam	λ, mW/m·K	T_g, °C	$T_{d,max1}$, °C	$T_{d,max2}$, °C	$T_{d,max3}$, °C	$T_{d,onset}$, °C
1-PU-diol	33.4	13	173	326	364	271
1-PU-triol	34.5	9	173	321	365	267
1-PU-tetraol	34.7	13	175	328	370	267
2-PU-diol	34.5	7	175	326	386	269
2-PU-triol	34.4	5	173	319	382	270
2-PU-tetraol	34.8	6	181	328		276
3-PU-diol	34.3	−28/21	178	328	401	280
3-PU-triol	34.4	−22/25	185	334	405	280
3-PU-tetraol	34.2	−23/25	177	328	408	283
REF	35.4	23	157	315	367	274

[a]Thermal conductivity coefficient (λ), glass transition temperature (T_g), and TGA results showing the temperatures of maximum decomposition ($T_{d,max}$) and the onset values of the second weight loss ($T_{d,onset}$) of the TG curves.

testing (Figure S9) and into samples with dimensions of approximately 200 mm × 200 mm × 40 mm for thermal conductivity (λ) coefficient determination. No shrinkage was observed in these large blocks of PUR foams even after 6 months (Figure S10), indicating excellent dimensional stability, especially considering the very low targeted foam density of ∼16 kg·m^{-3}.

The determined values of apparent density for all prepared foam samples closely approximated the target value, ranging from 15 to 17 kg·m^{-3} (Figure 3A). This places these foams in the category of ultralight materials, surpassing the majority of commercially available PUR foams.[39−41]

The production of such lightweight foams presents significant advantages from both economic and environmental perspectives. The substitution of the petrochemical-based polyol with a biobased alternative shows a minimal impact on foam density (Figure 3A). Although the inclusion of both types of biobased polyols (ETO-TMP and SA-polyols) in the foam formulation slightly reduced the apparent density as compared to the reference material, the differences between the PUR foams based on SA-polyols with different functionalities were negligible and statistically insignificant, as shown by the results of the one-way ANOVA test (Table S5).

The mechanical properties of the prepared foams were assessed by using a compression test. The stress−strain curves exhibited a primary linear relationship up to approximately 3% strain, followed by a sustained plateau region without a distinct yield point (Figure S11), a behavior characteristic of semirigid foams.[42] Figure 3B,C illustrates the normalized compressive modulus (E_{norm}) and compressive strength (σ_{norm}) of the PUR foams measured in the foam rise direction. In all three foam series, the E_{norm} and σ_{norm} values of the PUR foams were enhanced with the increased functionality of the SA-polyols used in their preparations. The statistical evaluations (the one-way ANOVA tests) of the compression data also confirmed the significant effect ($p < 0.001$) of the SA-polyol functionality for all three (1-PU, 2-PU, and 3-PU) series of PUR foams (Table S5). The improved compression properties of PUR foams are primarily attributed to the higher cross-link density resulting from the utilization of SA-polyols with a greater functionality. The PUR foams based solely on SA-polyols (3-PU series) exhibited the lowest compression properties due to the formation of diluted networks resulting from the absence of a higher functionality polyol. Conversely, the addition of 20% high-functionality polyol Lupranol 3422 significantly improved the compression properties of the PUR foams (1-PU series, Figure 3B,C). In the 1-PU series, the combination of SA-tetraol and Lupranol 3422 yielded PUR foams with E_{norm} and σ_{norm} values comparable to those of the reference PUR foam (REF) prepared using only commercial petrochemical polyols. However, the highest-performing PUR foam was achieved by incorporating a combination of two biopolyols, namely SA-polyols (particularly SA-triol and SA-tetraol) and ETO-TMP (2-PU series, Figure 3B,C). The 2-PU-tetraol foam demonstrated the highest compressive modulus (2.5 MPa) and compressive strength (64 kPa) without adversely affecting the foam density, which remained favorably low (16 kg·m^{-3}). Overall, the substitution of both petrochemical polyols with the synthesized biobased analogues resulted in improved mechanical properties of the PUR foams, attributable to the foam morphology. SEM observations (Figure 2) revealed that the PUR foams formulated exclusively with biopolyols exhibited a highly homogenous and fine cellular structure, contributing to their excellent mechanical properties[43] while maintaining a desirably low density.

Thermal Properties of Polyurethane Foams. Semirigid low-density PUR foams find typical application in thermal insulation for attics, walls, and ceilings.[44] In this context, the thermal conductivity (λ-coefficient) of the prepared PUR foams was determined to evaluate their thermal insulation properties. The thermal conductivity of PUR foams generally depends on factors such as foam density, cell size and anisotropy, the ratio of close to open cell content, and the thermal conductivity of the gases trapped within the cells.[45] In porous materials, conductive heat transfer primarily occurs through the gases present in the cells and solid medium.[46] In this study, the produced materials were characterized as low-density and partially open-cell PUR foams. Consequently, their thermal conductivity was predominantly influenced by the gas phase as the solid phase constituted only a minor fraction of the materials. In our case, the gas phase in all PUR foams consisted of carbon dioxide (λ_{CO_2} = 15.5 mW/m·K) generated during foaming as a blowing agent as well as air (λ_{Air} = 25.1 mW/m·K), which permeated into open cells and penetrated closed cells through cell membranes.[47] Due to the formulation similarities and open-cell content, the λ-values of all prepared PUR foams fell within a narrow range of 34.2−34.8 mW/m·K (Table 4). The inclusion of both types of biobased polyols led to an improvement in the thermal insulation properties, resulting in lower λ-values compared to the reference petroleum-based PUR foam (35.4 mW/m·K, Table 4) and other commercially available open-cell PUR foams (37−39 mW/m·K).[48]

https://doi.org/10.1021/acssuschemeng.3c06924
ACS Sustainable Chem. Eng. 2024, 12, 1605−1615

The exceptional thermal insulation properties of the PUR foams prepared from SA and ETO-TMP polyols become evident when compared to other PUR foams based on biobased polyols. It is noteworthy that biobased PUR foams with such a low thermal conductivity, while simultaneously exhibiting a partially open-cell structure, low density, and high mechanical strength, are rarely documented in the literature. For instance, Kuranska et al. reported the preparation of PUR foams with similar densities of approximately 14 kg·m^{-3} using polyols derived from epoxidized rapeseed oil.[49] These foams demonstrated comparable mechanical strength but inferior thermal insulation properties (the λ-coefficient of 38−41 mW/m·K). Similarly, the same research group prepared comparable PUR foams from transesterified vegetable oils.[50,51] Although these foams exhibited similar or even lower apparent density (12 kg·m^{-3}) and comparable compression strength, their thermal insulation ability was less efficient (the λ-coefficient of 36−44 mW/m·K), likely due to the more rough cellular structure and the presence of macroscopic defects such as voids.

The studies mentioned above have primarily focused on utilizing vegetable oil-derived polyols exclusively for the production of low-density open-cell PUR foams. However, PUR foams formulated solely with a single biocomponent, such as vegetable oil, tend to exhibit brittleness and low compressive strength. These inferior mechanical properties arise from the incorporation of short-chain and high-functionality polyols derived from vegetable oil, resulting in rigid and dense polymer networks. In this study, we employed a combination of two biobased polyols, the "rigid" and high-functional ETO-TMP derived from natural oil, along with the "flexible" and low-functional SA-polyols. This approach provided a possibility to achieve a suitable balance between hard and flexible chains within the PUR structure and enabled a consequent adjustment of the optimal cross-link density of the foams. The excellent compatibility of these biopolyols led to the formation of a single-phase microstructure in the fabricated PUR foams, as confirmed by DSC measurements revealing a single T_g value within the range of 5−13 °C (Table 4). This observation indicates the suppression of phase segregation into distinct hard and soft domains, promoting the development of a homogenous mixed-phase microstructure due to enhanced compatibility between the polyol and isocyanate components during foam formation and PUR network formation. In contrast, when only SA-polyols, which exhibited lower compatibility with pMDI, were utilized, the resulting PUR foams (the 3-PU series) displayed two distinct T_g values (Table 4), signifying microphase separation into soft (T_{g1} in the range of −28 to −22 °C) and hard (T_{g2} in the range of 21−25 °C) segments.

The differences in the T_g between 1-PU and 2-PU series were caused by different degrees of cross-linking in the PUR foams. Therefore, the 1-PU foams (based on the petrochemical polyol having a higher hydroxyl group content than that of ETO-TMP) exhibited higher T_g than that of the 2-PU foams. Moreover, all of the Lupranol hydroxyl groups are secondary, whereas in ETO-TMP, primary OH groups are also present. This can affect the mobility of the polymeric structures, resulting in higher T_g for foams based on the petrochemical polyol.[52]

Thermal stability assessment of the prepared PUR foams was conducted using TGA. The TG and DTG curves (Figure S12) of all the prepared PUR foams exhibited three distinct mass losses. The first, observed at temperatures below 250 °C ($T_{d\ max1}$ in Table 4), can be attributed to the volatilization of the TCPP fire retardant.[53] This initial step accounted for approximately 10 wt % of the material aligning well with the amount of TCPP added (see Table 1). The second and third weight loss steps were associated with decomposition of the PUR structure. The onset temperatures of the second weight loss ($T_{d,onset}$ in Table 4) fell within the range of 267−283 °C, indicating satisfactory thermal stability across all the PUR foams. Initially, the isocyanate-derived structures of PUR foams undergo breakdown, resulting in the formation of isocyanates, alcohols, primary or secondary amines, olefins, and carbon dioxide.[54] As the temperature continues to rise beyond 350 °C (the third weight loss), cleavage of the polyol-derived segments commences.[55,56]

Chemical Recycling/Solvolysis of Polyurethane Foams. The prepared PUR foams consist of permanent covalent networks, which render their physical recycling or reprocessing unfeasible. Typically, PUR foams can only be recycled through chemical methods that involve depolymerization, breaking down the PUR into oligomers and/or monomers.[57,58] Solvolysis, utilizing an appropriate reagent such as glycol to react with the cleavable urethane linkages in the PUR structure, represents one of the most promising chemical recycling approaches.[59,60] However, accessing these linkages can be challenging due to the steric hindrance imposed by the aromatic isocyanate-derived segments. In this study, the PUR foams have been deliberately designed to facilitate recycling/depolymerization through classical solvolysis or biorecycling methods involving enzymes or microorganisms, thanks to the presence of hydrolyzable ester bonds within the structure of SA-polyols.

The solvolysis process, specifically glycolysis, of PUR foams with incorporated SA-diol (1-PU-diol, 2-PU-diol, and 3-PU-diol) was studied and compared to reference foams (REF and REF_ETO-TMP) lacking degradable ester linkages. The recycling time, defined as the time required for a complete transformation of PUR foam pieces into the liquid state, was determined for microwave-assisted glycolysis using 4EG as the reagent. Our findings indicate that the inclusion of SA-diol in the foam formulation led to a reduction in recycling time, demonstrating the enhanced efficiency of glycolysis in these samples (Table 5).

The PUR foams containing 3-PU-diol and 1-PU-diol exhibited the shortest recycling times, which can be attributed to their more diluted network structure that allowed glycol molecules to readily access and react with the ester and urethane linkages. The slightly longer recycling time observed for the 2-PU-diol foam, which incorporated both SA-diol and ETO-TMP (Table 5), may be attributed to the steric hindrance caused by ETO-TMP, affecting the accessibility of the hydrolyzable linkages. However, it is important to note that the recycling time of the 2-PU-diol foam is still shorter than that of the reference foam REF, which does not contain degradable ester linkages. This is significant considering that the 2-PU-diol foam exhibits similar mechanical properties (Figure 3) and thus similar cross-link density. The recycling time of PUR foams appears to be influenced both by the degree of cross-linking and by the supramolecular structure of foam segments. It is evident that the more complex and branched structure of ETO-TMP polyol hinders the accessibility of glycol molecules to the ester and urethane linkages. This conclusion is further supported by additional

https://doi.org/10.1021/acssuschemeng.3c06924
ACS Sustainable Chem. Eng. 2024, 12, 1605−1615

Table 5. Glycolysis of Selected PUR Foams Using Various Amounts of Tetraethylene Glycol (4EG)[a]

PUR foam	4EG/PUR foam mass ratio	recycling time, s
1-PU-diol	2/1	80
	1.5/1	90
	1/1	100
2-PU-diol	2/1	110
	1.5/1	120
	1/1	140
3-PU-diol	2/1	85
	1.5/1	95
	1/1	105
REF	2/1	150
	1.5/1	170
	1/1	270
REF_ETO-TMP	2/1	190
	1.5/1	250
	1/1	n.d.[b]

[a]Recycling time was determined as a time necessary for a complete transformation of PUR foams into the liquid state. [b]Not determined, foam residue still visible after 10 min of glycolysis.

glycolysis experiments conducted with REF_ETO-TMP foam (Table 5), which is composed entirely of ETO-TMP polyol (detailed foam composition is provided in Table S2). The decomposition of the REF_ETO-TMP foam was the slowest, resulting in even longer recycling times compared to the REF foam (Table 5).

Clearly, the incorporation of SA-diols into the polyol structure of PUR foams facilitates the progress of glycolysis, allowing for a reduction in the amount of glycol required. This enables an efficient decrease in the mass ratio of 4EG to PUR foam with ratios as low as 1:1 (Table 5). By reducing the amount of the unreacted reagent that would otherwise have to be removed from the recycled product, the overall economics of the recycling process can be improved. Further analysis of the glycolysis products and their potential use for the preparation of novel PUR foams is outside the scope of this paper and will be the focus of our upcoming study.

CONCLUSIONS

Biobased aliphatic poly(ester-ether) polyols of different functionalities (2, 3, and 4) based on succinic acid (SA) and tetraethylene glycol have been synthesized. The incorporation of flexible ether linkages in the polyols suppressed crystallization tendencies, resulting in fully amorphous characteristics with low glass transition temperatures (T_g). These low-functional SA-polyols, alone or in combination with a biobased tall oil-derived polyol (ETO-TMP), were effectively utilized as replacements for petrochemical polyols in the preparation of ultralow-density polyurethane (PUR) foams. The resulting materials exhibited semirigid behavior with a partly open cellular structure and a favorable apparent density of 15−16 kg·m^{-3}. By combination of the rigid tall oil-derived polyols with the flexible SA-polyols, good compatibility among all PUR components was achieved, leading to the formation of a single-phase microstructure within the PUR foams. This allowed for a suitable balance of hard and flexible chains and an optimal cross-link density, resulting in PUR foams with homogenous and fine cellular structures, excellent mechanical properties, and low density.

Moreover, the incorporation of SA-polyols with hydrolyzable ester linkages enabled facile recycling of the PUR foams through solvolysis. The introduction of SA-diol into the PUR foam structure significantly accelerated the progress of glycolysis, making the recycling process up to 2.7 times faster. Additionally, the recycling time was influenced by the degree of cross-linking and the supramolecular structure of the PUR foam segments.

Overall, the 100% biopolyol-based PUR foams demonstrated outstanding structural and thermomechanical properties, while the incorporation of poly(ester-ether) polyols allowed for easy recyclability via solvolysis. Future work will focus on conducting a more detailed recycling study on the prepared PUR foams and exploring their potential for biorecycling.

ASSOCIATED CONTENT

Supporting Information

The Supporting Information is available free of charge at https://pubs.acs.org/doi/10.1021/acssuschemeng.3c06924.

Formulations of SA-based polyols and PUR foams, FTIR and MALDI-TOF spectra of SA-based polyols and PUR foams, SEM micrographs of PUR foams together with cell size distribution histograms and open cell content measurement results, PUR foam images, p values from a one-way ANOVA, and stress−strain, TG, DTG curves of PUR foams (PDF)

AUTHOR INFORMATION

Corresponding Author

Hynek Beneš − *Institute of Macromolecular Chemistry of the Czech Academy of Sciences, 162 00 Prague 6, Czech Republic;* orcid.org/0000-0002-6861-1997; Phone: +420 296 809 313; Email: benesh@imc.cas.cz

Authors

Olga Gotkiewicz − *Institute of Macromolecular Chemistry of the Czech Academy of Sciences, 162 00 Prague 6, Czech Republic*

Mikelis Kirpluks − *Polymer Laboratory, Latvian State Institute of Wood Chemistry, LV-1006 Riga, Latvia*

Zuzana Walterová − *Institute of Macromolecular Chemistry of the Czech Academy of Sciences, 162 00 Prague 6, Czech Republic*

Olga Kočková − *Institute of Macromolecular Chemistry of the Czech Academy of Sciences, 162 00 Prague 6, Czech Republic;* orcid.org/0000-0003-3761-4033

Sabina Abbrent − *Institute of Macromolecular Chemistry of the Czech Academy of Sciences, 162 00 Prague 6, Czech Republic;* orcid.org/0000-0003-4228-4059

Paulina Parcheta-Szwindowska − *Department of Polymer Technology, Faculty of Chemistry, Gdansk University of Technology, 80-233 Gdansk, Poland;* orcid.org/0000-0003-3337-6023

Ugis Cabulis − *Polymer Laboratory, Latvian State Institute of Wood Chemistry, LV-1006 Riga, Latvia*

Complete contact information is available at: https://pubs.acs.org/10.1021/acssuschemeng.3c06924

Author Contributions

The article was written through contributions of all authors. All authors have given approval to the final version of the article.

Funding

This work was supported by the Czech Academy of Sciences and the Latvian Academy of Sciences (mobility project no. LZA-22-02 "Innovative Bio-based Polyols and Advanced Methods of Their Characterization").

Notes

The authors declare no competing financial interest.

REFERENCES

(1) Plastics Europe. *Plastics - the Facts 2022*; 2022. https://plasticseurope.org/knowledge-hub/plastics-the-facts-2022/ (accessed July 11, 2022).

(2) Morici, E.; Dintcheva, N. T. Recycling of Thermoset Materials and Thermoset-Based Composites: Challenge and Opportunity. In *Polymers*; MDPI, October 1, 2022.

(3) Statista. *Market volume of polyurethane worldwide from 2015 to 2022, with a forecast for 2023 to 2030*. https://www.statista.com/statistics/720341/global-polyurethane-market-size-forecast/ (accessed Oct 18, 2023).

(4) Kemona, A.; Piotrowska, M. Polyurethane Recycling and Disposal: Methods and Prospects. In *Polymers*; MDPI AG, August 1, 2020.

(5) Acumen Research and Consulting. *Microcellular Polyurethane Foam Market Size - Global Industry Share, Analysis, Trends and Forecast 2022 - 2030*. https://www.acumenresearchandconsulting.com/microcellular-polyurethane-foam-market (accessed Aug 15, 2022).

(6) DATAINTELO. *Low Density Microcellular Polyurethane Foam Market Research Report 2021−2028*. https://dataintelo.com/report/global-microcellular-polyurethane-foam-sales-market/ (accessed Aug 15, 2022).

(7) Guo, B.; Pierron, F.; Rotinat, R. In *Identification of Low Density Polyurethane Foam Properties by DIC and the Virtual Fields Method*, ICEM 2008: International Conference on Experimental Mechanics; SPIE, 2008; Vol. *7375*, 737554.

(8) Marcovich, N. E.; Kurańska, M.; Prociak, A.; Malewska, E.; Kulpa, K. Open Cell Semi-Rigid Polyurethane Foams Synthesized Using Palm Oil-Based Bio-Polyol. *Ind. Crops Prod* **2017**, *102*, 88−96.

(9) Wang, G.; Yang, T. Preparation of Open Cell Rigid Polyurethane Foams and Modified with Organo-Kaolin. *J. Cell. Plast.* **2020**, *56* (4), 435−447.

(10) Olazabal, I.; González, A.; Vallejos, S.; Rivilla, I.; Jehanno, C.; Sardon, H. Upgrading Polyurethanes into Functional Ureas through the Asymmetric Chemical Deconstruction of Carbamates. *ACS Sustainable Chem. Eng.* **2023**, *11* (1), 332−342.

(11) Beneš, H.; Vlčková, V.; Paruzel, A.; Trhlíková, O.; Chalupa, J.; Kanizsová, L.; Skleničková, K.; Halecký, M. Multifunctional and Fully Aliphatic Biodegradable Polyurethane Foam as Porous Biomass Carrier for Biofiltration. *Polym. Degrad. Stab.* **2020**, *176*, No. 109156.

(12) Skleničková, K.; Abbrent, S.; Halecký, M.; Kočí, V.; Beneš, H. Biodegradability and Ecotoxicity of Polyurethane Foams: A Review. In *Critical Reviews in Environmental Science and Technology*; Taylor and Francis Ltd., 2022; pp 157−202.

(13) Nilawar, S.; Chatterjee, K. Olive Oil-Derived Degradable Polyurethanes for Bone Tissue Regeneration. *Ind. Crops Prod.* **2022**, *185*, No. 115136.

(14) Skleničková, K.; Vlčková, V.; Abbrent, S.; Bujok, S.; Paruzel, A.; Kanizsová, L.; Trhlíková, O.; Říhová Ambrožová, J.; Halecký, M.; Beneš, H. Open-Cell Aliphatic Polyurethane Foams with High Content of Polysaccharides: Structure, Degradation, and Ecotoxicity. *ACS Sustainable Chem. Eng.* **2021**, *9* (17), 6023−6032.

(15) Trhlíková, O.; Vlčková, V.; Abbrent, S.; Valešová, K.; Kanizsová, L.; Skleničková, K.; Paruzel, A.; Bujok, S.; Walterová, Z.; Innemanová, P.; Halecký, M.; Beneš, H. Microbial and Abiotic Degradation of Fully Aliphatic Polyurethane Foam Suitable for Biotechnologies. *Polym. Degrad. Stab.* **2021**, *194*, No. 109764, DOI: 10.1016/j.polymdegradstab.2021.109764.

(16) Kirpluks, M.; Kalnbunde, D.; Benes, H.; Cabulis, U. Natural Oil Based Highly Functional Polyols as Feedstock for Rigid Polyurethane Foam Thermal Insulation. *Ind. Crops Prod.* **2018**, *122*, 627−636.

(17) Sardon, H.; Mecerreyes, D.; Basterretxea, A.; Avérous, L.; Jehanno, C. From Lab to Market: Current Strategies for the Production of Biobased Polyols. *ACS Sustainable Chem. Eng.* **2021**, 10664−10677, DOI: 10.1021/acssuschemeng.1c02361.

(18) Nghiem, N. P.; Kleff, S.; Schwegmann, S. Succinic Acid: Technology Development and Commercialization. In *Fermentation*; MDPI AG, June 1, 2017.

(19) Li, C.; Ong, K. L.; Cui, Z.; Sang, Z.; Li, X.; Patria, R. D.; Qi, Q.; Fickers, P.; Yan, J.; Lin, C. S. K. Promising Advancement in Fermentative Succinic Acid Production by Yeast Hosts. *J. Hazard. Mater.* **2021**, *401*, No. 123414.

(20) Akhtar, J.; Idris, A.; Abd Aziz, R. Recent Advances in Production of Succinic Acid from Lignocellulosic Biomass. *Appl. Microbiol. Biotechnol.* **2014**, 987−1000, DOI: 10.1007/s00253-013-5319-6.

(21) Werpy, T.; Petersen, G. *Top Value Added From Biomass; Volume I: Results of Screening for Potential Candidates from Sugars and Synthesis Gas*; 2004. http://www.osti.gov/bridge (accessed July 11, 2022).

(22) Saxena, R. K.; Saran, S.; Isar, J.; Kaushik, R. Production and Applications of Succinic Acid. In *Current Developments in Biotechnology and Bioengineering: Production, Isolation and Purification of Industrial Products*; Elsevier Inc., 2016; pp 601−630.

(23) Marcovich, N. E.; Kurańska, M.; Prociak, A.; Malewska, E.; Bujok, S. The Effect of Different Palm Oil-Based Bio-Polyols on Foaming Process and Selected Properties of Porous Polyurethanes. *Polym. Int.* **2017**, *66* (11), 1522−1529.

(24) Polaczek, K.; Kurańska, M.; Auguścik-Królikowska, M.; Prociak, A.; Ryszkowska, J. Open-Cell Polyurethane Foams of Very Low Density Modified with Various Palm Oil-Based Bio-Polyols in Accordance with Cleaner Production. *J. Cleaner Prod.* **2021**, *290*, No. 125875.

(25) Kirpluks, M.; Vanags, E.; Abolins, A.; Michalowski, S.; Fridrihsone, A.; Cabulis, U. High Functionality Bio-Polyols from Tall Oil and Rigid Polyurethane Foams Formulated Solely Using Bio-Polyols. *Materials* **2020**, *13* (8), No. 1985.

(26) Hawkins, M. C.; O'Toole, B.; Jackovich, D. Cell Morphology and Mechanical Properties of Rigid Polyurethane Foam. *J. Cell. Plast.* **2005**, *41* (3), 267−285.

(27) Rajput, B. S.; Hai, T. A. P.; Gunawan, N. R.; Tessman, M.; Neelakantan, N.; Scofield, G. B.; Brizuela, J.; Samoylov, A. A.; Modi, M.; Shepherd, J.; Patel, A.; Pomeroy, R. S.; Pourahmady, N.; Mayfield, S. P.; Burkart, M. D. Renewable Low Viscosity Polyester-Polyols for Biodegradable Thermoplastic Polyurethanes. *J. Appl. Polym. Sci.* **2022**, *139* (43), No. e53062, DOI: 10.1002/app.53062.

(28) Ionescu, M. *Chemistry and Technology of Polyols for Polyurethanes*; Smithers Rapra Technology, 2005; p 542.

(29) ROQUETTE. *POLYESTER* POLYOLS AND *THERMOPLASTIC POLYURETHANES DATASHEET*. https://www.roquette.com/-/media/documentation/biosuccinium/data-sheets/roquette-biosuccinium-datasheet-polyester-polyols-and-thermoplastic-polyurethanes-2021-08-2684.pdf (accessed May 20, 2023).

(30) de Luca Bossa, F.; Verdolotti, L.; Russo, V.; Campaner, P.; Minigher, A.; Lama, G. C.; Boggioni, L.; Tesser, R.; Lavorgna, M. Upgrading Sustainable Polyurethane Foam Based on Greener Polyols: Succinic-Based Polyol and Mannich-Based Polyol. *Materials* **2020**, *13* (14), No. 3170.

(31) Ionescu, M.; Petrović, Z. S. High Functionality Polyether Polyols Based on Polyglycerol. *Journal of Cellular Plastics* **2010**, *46* (3), 223−237.

(32) Obi, B. E. Foaming Processes. In *Polymeric Foams Structure-Property-Performance*; Elsevier, 2018; pp 131−188.

(33) Quinsaat, J. E. Q.; Feghali, E.; Van De Pas, D. J.; Vendamme, R.; Torr, K. M. Preparation of Mechanically Robust Bio-Based Polyurethane Foams Using Depolymerized Native Lignin. *ACS Appl. Polym. Mater.* **2021**, *3* (11), 5845−5856.

(34) Głowińska, E.; Gotkiewicz, O.; Kosmela, P. Sustainable Strategy for Algae Biomass Waste Management via Development of Novel Bio-Based Thermoplastic Polyurethane Elastomers Composites. *Molecules* **2023**, *28* (1), No. 436.
(35) Papadopoulos, E.; Ginic-Markovic, M.; Clarke, S. A Thermal and Rheological Investigation during the Complex Cure of a Two-Component Thermoset Polyurethane. *J. Appl. Polym. Sci.* **2009**, *114* (6), 3802−3810.
(36) Lim, H.; Kim, S. H.; Kim, B. K. Effects of the Hydroxyl Value of Polyol in Rigid Polyurethane Foams. *Polym. Adv. Technol.* **2008**, *19* (12), 1729−1734.
(37) Cantat, I.; Cohen-Addad, S.; Elias, F.; Graner, F.; Höhler, R.; Pitois, O.; Rouyer, F.; Saint-Jalmes, A. *Foams: Structure and Dynamics*, 1st ed.; Cox, S., Ed.; Oxford University Press: Oxford, 2013.
(38) Fan, H.; Tekeei, A.; Suppes, G. J.; Hsieh, F. H. Rigid Polyurethane Foams Made from High Viscosity Soy-Polyols. *J. Appl. Polym. Sci.* **2013**, *127* (3), 1623−1629.
(39) Easycomposites. *easycomposites PU Foam, Model Board & Tooling Board*. https://www.easycomposites.co.uk/model-board-tooling-board-block (accessed May 20, 2023).
(40) DUNA-Group. *CORAFOAM Low density*. https://www.dunagroup.com/usa/products/foams/corafoam-low-density (accessed May 20, 2023).
(41) W., Dimer GmbH. *PUR foam/polyurethane foam Collar*. https://www.dimer.com/en/Materials/pur-flexible-foam/pur-foam.html (accessed May 20, 2023).
(42) Linul, E.; Vălean, C.; Linul, P. A. Compressive Behavior of Aluminum Microfibers Reinforced Semi-Rigid Polyurethane Foams. *Polymers* **2018**, *10* (12), No. 1298.
(43) Prociak, A.; Kurańska, M.; Cabulis, U.; Ryszkowska, J.; Leszczyńska, M.; Uram, K.; Kirpluks, M. Effect of Bio-Polyols with Different Chemical Structures on Foaming of Polyurethane Systems and Foam Properties. *Ind. Crops Prod.* **2018**, *120*, 262−270.
(44) Polaczek, K.; Kurańska, M.; Prociak, A. Open-Cell Bio-Polyurethane Foams Based on Bio-Polyols from Used Cooking Oil. *J. Cleaner Prod.* **2022**, *359*, No. 132107.
(45) Thirumal, M.; Khastgir, D.; Singha, N. K.; Manjunath, B. S.; Naik, Y. P. Effect of Foam Density on the Properties of Water Blown Rigid Polyurethane Foam. *J. Appl. Polym. Sci.* **2008**, *108* (3), 1810−1817.
(46) Choe, H.; Choi, Y.; Kim, J. H. Threshold Cell Diameter for High Thermal Insulation of Water-Blown Rigid Polyurethane Foams. *J. Ind. Eng. Chem.* **2019**, *73*, 344−350.
(47) Kirpluks, M.; Godina, D.; Švajdlenková, H.; Šauša, O.; Modniks, J.; Simakovs, K.; Andersons, J. Effect of Crosslink Density on Thermal Aging of Bio-Based Rigid Low-Density Closed-Cell Polyurethane Foams. *ACS Appl. Polym. Mater.* **2023**, *5*, No. 4305.
(48) Kurańska, M.; Barczewski, R.; Barczewski, M.; Prociak, A.; Polaczek, K. Thermal Insulation and Sound Absorption Properties of Open-Cell Polyurethane Foams Modified with Bio-Polyol Based on Used Cooking Oil. *Materials* **2020**, *13* (24), No. 5673.
(49) Kurańska, M.; Polaczek, K.; Auguścik-Królikowska, M.; Prociak, A.; Ryszkowska, J. Open-Cell Rigid Polyurethane Bio-Foams Based on Modified Used Cooking Oil. *Polymer* **2020**, *190*, No. 122164.
(50) Kurańska, M.; Malewska, E.; Polaczek, K.; Prociak, A.; Kubacka, J. A Pathway toward a New Era of Open-Cell Polyurethane Foams—Influence of Bio-Polyols Derived from Used Cooking Oil on Foams Properties. *Materials* **2020**, *13* (22), No. 5161.
(51) Kamińska, K.; Barczewski, M.; Kurańska, M.; Malewska, E.; Polaczek, K.; Prociak, A. The Effect of a Chemical Foaming Agent and the Isocyanate Index on the Properties of Open-Cell Polyurethane Foams. *Materials* **2022**, *15* (17), No. 6087.
(52) Camara, F.; Benyahya, S.; Besse, V.; Boutevin, G.; Auvergne, R.; Boutevin, B.; Caillol, S. Reactivity of Secondary Amines for the Synthesis of Non-Isocyanate Polyurethanes. *Eur. Polym. J.* **2014**, *55* (1), 17−26.
(53) Kurańska, M.; Beneš, H.; Sałasińska, K.; Prociak, A.; Malewska, E.; Polaczek, K. Development and Characterization of "Green Open-Cell Polyurethane Foams" with Reduced Flammability. *Materials* **2020**, *13* (23), No. 5459.
(54) Sui, H.; Ju, X.; Liu, X.; Cheng, K.; Luo, Y.; Zhong, F. Primary Thermal Degradation Effects on the Polyurethane Film. *Polym. Degrad. Stab.* **2014**, *101* (1), 109−113.
(55) Chattopadhyay, D. K.; Webster, D. C. Thermal Stability and Flame Retardancy of Polyurethanes. *Prog. Polym. Sci.* **2009**, *34*, 1068−1133.
(56) Trovati, G.; Sanches, E. A.; Neto, S. C.; Mascarenhas, Y. P.; Chierice, G. O. Characterization of Polyurethane Resins by FTIR, TGA, and XRD. *J. Appl. Polym. Sci.* **2010**, *115* (1), 263−268.
(57) Wang, X.; Chen, H.; Chen, C.; Li, H. Chemical Degradation of Thermoplastic Polyurethane for Recycling Polyether Polyol. *Fibers Polym.* **2011**, *12* (7), 857−863.
(58) Paruzel, A.; Michałowski, S.; Hodan, J.; Horák, P.; Prociak, A.; Beneš, H. Rigid Polyurethane Foam Fabrication Using Medium Chain Glycerides of Coconut Oil and Plastics from End-of-Life Vehicles. *ACS Sustainable Chem. Eng.* **2017**, *5* (7), 6237−6246.
(59) Beneš, H.; Rösner, J.; Holler, P.; Synková, H.; Kotek, J.; Horák, Z. Glycolysis of Flexible Polyurethane Foam in Recycling of Car Seats. *Polym. Adv. Technol.* **2007**, *18* (2), 149−156.
(60) Jutrzenka Trzebiatowska, P.; Beneš, H.; Datta, J. Evaluation of the Glycerolysis Process and Valorisation of Recovered Polyol in Polyurethane Synthesis. *React. Funct Polym.* **2019**, *139*, 25−33.